論文の内容の要旨

New hydrogen-ordered phase and proton dynamics of ice revealed by dielectric and neutron diffraction measurements using newly developed high pressure cells

（誘電率および中性子回折測定用の高圧セル開発による
氷高圧相の新しい秩序相の発見とプロトンダイナミクスの解明）

氏名：山根　崚

Ice is the most fundamental molecular solid in the large material group, such as confined water and hydrates, characterized by water molecules. Nineteen ice polymorphs have been reported so far. The polymorphs can be classified into hydrogen disordered and hydrogen-ordered phases, where hydrogen atoms occupy their sites at 50 and 100%, respectively. These states include some notable physical phenomena, such as a residual entropy caused by ice rule. In this thesis, I studied two unresolved problems of disordered high-pressure phases, ice VI and VII appearing at 1–2 GPa and 2–60 GPa, respectively. Salzmann et al. (2009) found that impurity-doping induces a phase transition to its ordered phase, ice XV, using neutron diffraction. Recently, the existence of another ordered phase was suggested in addition to ice XV (Gasser et al., 2018). Anomalous behavior of ice VII, on the other hand, has been reported around 10 GPa. For example, Pruzan et al. (1990) reported that a width of a Raman band of a symmetric stretching mode of a water molecule, has a minimum at around 10 GPa. Somayazulu et al. (2008) showed a peak splitting in an X-ray diffraction pattern at 14.8 GPa. Okada et al. (2014) showed that DC electric conductivity of ice VII has a maximum at 12 GPa from impedance measurements. However, no comprehensive interpretation for the experimental anomalies has been found.

Chapter 2 describes the discovery of a new hydrogen-ordered phase of ice VI, named as

ice XIX, from in situ of dielectric and neutron diffraction measurements at high pressure. Ice XV has been known as a hydrogen-ordered phase of ice VI so far. This is the second discovery of hydrogen-ordered phase of ice VI. Representative data of temperature dependence of dielectric loss and neutron diffraction of ice VI and ice XIX are shown in Fig. 1. Hydrogen ordering was observed as disappearance of dielectric response at 117 K (Fig. 1(a)) and as appearance of new peaks in the diffraction pattern at 108 K (Fig. 1(b)). These phenomena were caused by a limitation of reorientation of water molecules and symmetry lowering accompany with the hydrogen-ordering. Furthermore, structure analysis of ice XIX clarified that its unit cell is expanded to $\sqrt{2} \times \sqrt{2} \times 1$ from a unit cell of ice VI. I also proposed the two most possible structure models for ice XIX whose space groups are $P\bar{4}$ or $Pcc2$.

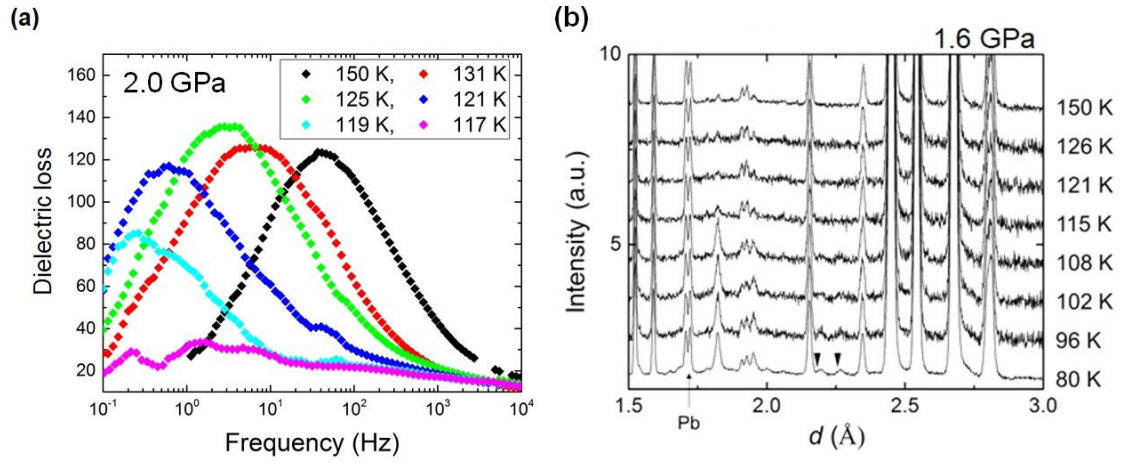

FIG. 1: (a) Temperature dependence of dielectric loss of ice VI and its new ordered phase at 2.0 GPa. (b) Neutron diffraction patterns obtained at 1.6 GPa and temperatures between 80–150 K. Pb, pressure marker, shows a peak at around 1.75 Å. The black triangle ticks indicate that their corresponding peaks are derived from $\sqrt{2} \times \sqrt{2} \times 1$ unit cell of a new ordered phase of ice VI. Hydrogen disorder-order transition can be seen at around 120 K in both measurements.

Chapter 3 describes investigation of dielectric properties of ice VII beyond 10 GPa using a newly developed high-pressure cell. As a result, a theoretically predicted scenario was observed (Hernandez and Caracas, 2018); dominant dynamics of disordered state of ice VII changes from molecular rotation to proton translation at

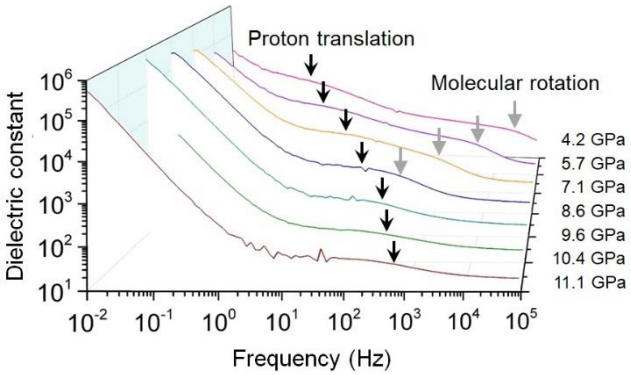

FIG. 2: Pressure dependence of dielectric constant of ice VII. Black and grey arrows indicate dielectric relaxations with their dynamics.

around 10 GPa. Figure 2 shows the dynamics crossover observed in my dielectric experiments. Two dielectric relaxations were observed below 8.6 GPa, and the expected pressure response was observed considering activation volume of the each dynamics; molecular rotation was inactivated and proton translation was activated with increasing pressure. The two dielectric relaxations merged at around 10 GPa on the frequency axis, and the dielectric relaxation of proton translation is faster than that of water rotation above the pressure. This result is the direct observation of the theoretically predicted dynamics crossover in ice VII. My study gives the solution to the reported anomalous behavior of ice VII at around 10 GPa with the theoretical report (Hernandez and Caracas, 2018).

Chapter 4 describes neutron diffraction experiments of ice VII carried out under high pressure and high electric field for search of a ferroelectrically (abbreviated FE) ordered structure of ice VII. Coexistence of FE ordered domain in ice VII was also theoretically suggested as an interpretation for the anomalous behavior of ice VII at around 10 GPa (Caracas and Hemley, 2015). This is the first case of neutron experiments under the multi-extreme conditions. As a result, no clear evidence of the appearance of the FE ordered structure of ice VII was obtained from the observed diffraction patterns as shown in Fig. 3. Although further technical improvements would be necessary to find the potential existence FE structure, this study will be continued for the aim of the discovery of FE ordered structure by applying much higher electric field. The discovery should have a high impact considering its notable structural property in contrast to a typical antiferroelectrically ordered structure, ice VIII, which is an ordered phase of ice VII.

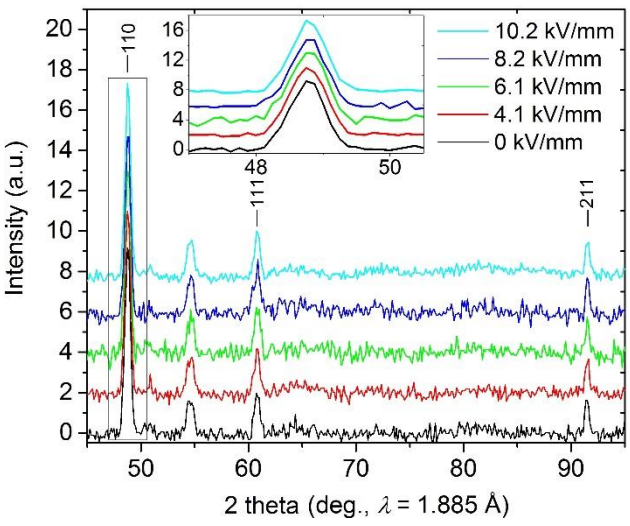

FIG. 3: Neutron diffraction patterns at 6.2 GPa and with electric fields of 0, 4.1, 6.1, 8.2, and 10.2 kV/mm. Exposure times were 1, 1, 0.5, 0.5, and 2 h, respectively. The inset shows expanded plots at around 50°. From lower angle, 110, 111, and 211 reflections of ice VII are observed. The peak at around 55° is 110 reflection of diamond (anvils). The undulation from 60° to 90° couldbe derived from inhomogeneous gaps of the radial collimator partitions.

Chapter 5 describes technical developments for high-pressure dielectric experiments.

Figure 4(a) and (b) show the two developed cells. These cells are used depending on target pressures; one of them is a piston-cylinder type and the other one is a Bridgman type cell. Their achievable pressures are up to 2.5 GPa and 13 GPa, respectively. Sample pressure can be estimated from in situ ruby fluorescence measurement. A notable feature of the cells is that they are applicable to not only solid samples but also liquid samples by overcoming technical difficulties, such as maintaining electrodes in parallel under high pressure.

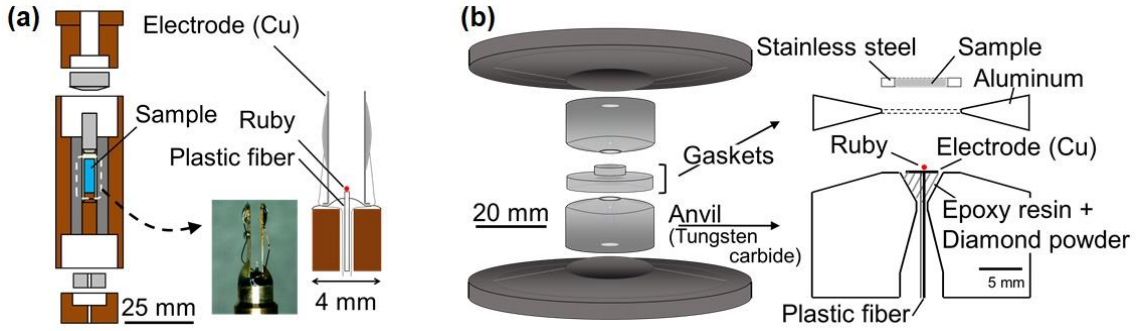

FIG. 4: Cell assemblies of piston-cylinder and Bridgman type high-pressure apparatuses for dielectric measurements, shown in (a) and (b), respectively. Samples are loaded vertically and their pressures are estimated using ruby fluorescence method.

In conclusion, I clarified the two unresolved problems of high-pressure phases of ice, VI and VII using newly developed high-pressure cells. I found the new ordered phase of ice VI besides the known ordered phase, ice XV. This is the first study revealing that one disordered ice has two hydrogen-ordered phases. This one-to-many correspondence opens new avenues to investigate the diversity of ice. For the anomalous behavior of ice VII at around 10 GPa, I directly observed that dominant dynamics of disordered state of ice VII changes from molecular rotation to proton translation. The first observation of the proton dynamics gives an experimental insight in light of its pressure response for not only ice but also other substances, such as proton conductors. As a different approach for the anomalous behavior of ice VII, I studied the search for a FE ordered structure of ice VII using neutron diffraction under high pressure and high electric field. Although I have not found out the FE ordered structure yet, my original experiment motivates other future works aiming to open a new research field of ice using electric field, such as an electric field induced new phase of ice.